

Friction and Wear Characteristics of Hot-Pressed NiCr–Mo/MoO₃/Ag Self-Lubrication Composites at Elevated Temperatures up to 900 °C

Jian-Yi Wang^{1,2} · Yu Shan¹ · Hongjian Guo^{1,2} · Bo Li¹ · Wenzhen Wang¹ · Junhong Jia¹

Received: 7 February 2015 / Accepted: 1 August 2015 / Published online: 13 August 2015
© Springer Science+Business Media New York 2015

Abstract NiCr-based high-temperature self-lubricating composites with Ag/Mo/Ag–MoO₃/Ag–Mo were prepared by the powder metallurgy method, respectively. The mechanical and tribological properties of the composites rubbing against alumina balls were investigated from room temperature to 900 °C. The tribo-chemical reaction films formed on the sliding surface and their effects on the tribological properties of composites at different temperatures were analyzed by SEM and Micro-Raman. The results showed that the tribological properties of NiCr-based composites were improved by adding alloying elements or a solid lubricating phase; meanwhile, the composites containing Ag–MoO₃ or Ag–Mo exhibited even better tribological properties than those with Mo or Ag at high temperatures. The lowest friction coefficient of the NiCr–MoO₃–Ag composite is around 0.19 and that of the NiCr–Mo–Ag composite is around 0.20; both composites exhibited an optimal wear rate in the order of magnitude of 10^{−6} mm³ N^{−1} m^{−1} at high temperatures. XRD and Micro-Raman results indicated that the composition of the tribo-layers formed on the worn surface of the composites varies with different testing temperatures. Compounds such as Ag₂MoO₄, NiCr₂O₄ and NiO, which formed on the rubbing surface at high temperature, worked synergistically to improve the tribological properties of the NiCr-based composite at high temperatures.

Keywords NiCr-based composite · Tribological properties · High temperature · Tribo-chemical reaction

1 Introduction

In recent decades, achieving as well as maintaining low friction and wear at high temperatures (>700 °C up to 1000 °C) has remained one of the most challenging problems encountered in the field of tribology [1–5], especially with the development of new-generation gas turbine engines, advanced jet engines and powder-generating systems, which require increasingly high temperatures (at 800 °C or even 1000 °C). Generally, using a single lubricant can only provide effective lubrication in a limited range of conditions. For example, conventional solid lubricants, such as graphite and molybdenum disulfide, lose the lubricating effects above 500 °C because of the inadequate oxidation resistance in air [6, 7]. Oxides, fluorides and some inorganic acid salts such as high-temperature solid lubricants cannot be used at low temperature [6]. Soft noble metals, such as silver, cannot provide effective lubrication above 500 °C because of excessive softening [8]. It is urgent to search for efficient solid lubricants or novel high-temperature self-lubricating materials possessing favorable frictional properties and wear resistance abilities that can serve at higher temperatures. Studies have found that nickel-based composites containing solid lubricants can be used effectively in new-generation high-performance gas turbine engines because of their excellent self-lubricating properties over an extreme range of operating temperatures [7, 9, 10]. It has also been found that the combination of two or more lubricants containing low- and high-temperature lubricants can improve the temperature adaptability of nickel-based composites [11–14]. Researchers at NASA

✉ Junhong Jia
jhjia@licp.cas.cn

¹ State Key Laboratory of Solid Lubrication, Lanzhou Institute of Chemical Physics, Chinese Academy of Sciences, Lanzhou 730000, People's Republic of China

² University of Chinese Academy of Sciences, Beijing 100039, People's Republic of China

have developed a series of plasma-sprayed (PS200, PS300, PS304 and PS400) and powder metallurgy high-temperature, self-lubricating materials (PM212, PM300 and PM304) with favorable tribological properties over broad temperature ranges [15–19]. In these composites, a Ni-based alloy as the matrix and silver and BaF₂/CaF₂ eutectic as solid lubricants, all of these composites exhibited low friction from room temperature to 650 °C. However, the decline of mechanical properties and oxidation of the coating deteriorated its wear resistance when the temperature was above 800 °C [18]. Furthermore, the wear rate of the PS coating in the range of 10⁻⁴–10⁻³ mm³ N⁻¹ m⁻¹ at room temperature was still relatively high for application.

To extend the applied temperature range and temperature adaptability of lubricating materials, the synergetic effects of the combination of transition metals (Mo, Cr, Nb, etc.) and soft metals (Ag, Cs, Pb, etc.) and the lubrication mechanisms of Ag–Mo, Cs–Mo, Pb–Mo and Cu–Mo, etc., from 25 to 700 °C in a single composite material were investigated [20–22]. For example, Muratore [22–24] deposited an adaptive YSZ–Ag–Mo coating (prepared by MS and PLD), which could provide lubrication by the formation of a continuous silver film on the worn surface at moderate temperatures (below 500 °C) and lubricious MoO₃ compounds in the wear track at high temperatures (above 500 °C). Chen [21] prepared a NiCrAlY–Ag–Mo composite coating APS, which displayed good tribological properties from 20 to 800 °C; the friction coefficients were around 0.3 and wear rates on the order of 10⁻⁵ mm³ · N⁻¹ m⁻¹. They proposed that the silver provides lubrication at temperatures below 400 °C; silver molybdate and MoO₃ act as lubricants at higher temperature (above 400 °C). Gulbinski [25] first reported the high temperature lubricity of silver molybdate, which was then further researched by Muratore and Voevodin [22, 23]. Our previous study on the lubricating behavior of Ag₂MoO₄ in Ni-based composites showed that relatively good tribological properties of composites could be achieved up to 700 °C [26]. The lowest friction coefficient and wear rate were [(0.26) and 1.02 × 10⁻⁵ mm³ N⁻¹ m⁻¹], respectively. The lubricating property of molybdate at even higher temperatures than 700 °C has not been investigated. Meanwhile, the poor mechanical properties of the composites (the Vickers hardness is lower than 170) are a serious problem. Many positive results have been achieved by combining low- and high-temperature lubricants [21, 22, 25, 26]. However, studies of the synergetic effects of the combination of transition metals and soft metals have been almost entirely confined to composite coatings [21–23, 25]. Moreover, it has been proposed that in the lubricant combination of Mo–Ag, Mo was first oxidized to molybdenum oxide during high temperature sliding. The molybdenum oxide compounds combined with silver

molybdate formed by the tribo-chemical reaction acted as high-temperature lubricants to provide high-temperature lubrication for the composite coatings. Thus, the feasibility of direct MoO₃ incorporation rather than Mo in the composites was further studied in the work, but the related study has not been reported yet. Driven by the above two aspects, the goal of this article is to fabricate Ni-based high-temperature self-lubricating composites containing Ag–Mo and Ag–MoO₃ and conduct comprehensive research on the tribological properties of the composites from room temperature to 900 °C. Meanwhile, Ni-based composites with Ag or Mo have also been studied. This is expected to clarify the effect and different lubrication mechanisms of Ag–Mo and Ag–MoO₃ in NiCr-based composites by comparison. In these composites, the NiCr matrix offers good mechanical and antioxidizing properties at high temperature. Ag acts as a low-temperature lubricant below 500 °C and is expected to form a tribolayer with silver molybdate as a high-temperature lubricant by tribo-chemical reaction at high temperatures to achieve low friction coefficients and wear rates in a wide temperature range.

2 Materials and Methods

2.1 Preparation of Ni-Based Composites

The Ni-based composites with 10 wt% Ag, 10 wt% Mo, 10 wt% Ag-10 wt% MoO₃ and 10 wt% Ag-10 wt% Mo were respectively prepared by the powder metallurgical hot-pressing method, denoted as NC (without additions), NCA (with Ag), NCM (with Mo), NCAM (with Ag and Mo) and NCAMO (with Ag and MoO₃). Commercially available nickel, chromium, molybdenum trioxide, molybdenum and silver powders were used as the starting materials of the matrix. The compositions of the Ni-based composites are given in Table 1. The Ni (80 wt%) and Cr (20 wt%) powders with mean particle sizes of 30–70 μm were first mixed for 20 h in a high-energy-mill (Fritsch, Germany). Then Ag powder, Mo powder, Ag–MoO₃ powder or Ag–Mo powder with a mean particle size of 5–20 μm was added and continuously ball-milled for 10 h. The composite powders were enclosed in a graphite die and set in a vacuum-hot-pressing furnace (ZT-45-20Y, China). When the furnace was evacuated to a dynamic vacuum of about 10⁻² Pa, the furnace was heated at a rate of 10 °C min⁻¹, and the powders were first pressed at 800 °C and held at constant temperature for 30 min under 25 MPa pressure. Then the heating of the furnace continued to 1100 °C (at a rate of 10 °C min⁻¹) and was held constant at this temperature for 30 min under 25 MPa pressure. The prefabricated specimens were machined to the desired

Table 1 Composition, preparation technology, density and Vickers hardness of the hot-pressed Ni-based composites

Ni-based composites	Composition (wt%)				Preparation technology	Density (g cm^{-3})	Vickers hardness (HV)
	80Ni–20Cr	Ag	MoO ₃	Mo			
NC	Balance	0	0	0	800 °C/1100 °C/ 30 min/25 MPa	8.21	232.41 ± 3.52
NCM	Balance	0	0	10	Same above	8.30	319.35 ± 3.73
NCA	Balance	10	0	0	Same above	8.32	210.35 ± 4.83
NCAM	Balance	10	10	0	Same above	8.27	281.53 ± 1.52
NCAMO	Balance	10	0	10	Same above	7.85	285.55 ± 5.98

samples and polished by emery paper for the following tests. The roughness values of the polished surfaces were about 0.3–0.5 μm (Ra).

2.2 Characterization

The phase compositions of the composites were examined by X-ray diffraction (XRD) on a Rigaku D/max-RB X-ray diffractometer utilizing Cu K α radiation with 40-kV operating voltage and a scan speed of $10^\circ \text{ min}^{-1}$ in the 2θ range of 10–80°. The microstructure and morphologies of worn surfaces were characterized by a JSM-5600LV scanning electron microscope (SEM) equipped with energy dispersive spectroscopy (EDS). The variations of the phase compositions on worn surfaces were investigated by a Renishaw inVia Micro-Raman spectroscopy using a laser light with 633-nm wavelength. The nanoindentation experiments were performed on a TI 950 Nano Mechanical Test Instrument (Hysitron, Minneapolis, MN, USA) to analyze the hardness of the glaze layers formed on the worn surfaces.

The Vicker hardness was measured by MH-5 Vicker's indentation using a normal load of 300 g and dwell time of 10 s. The measurements were carried out at least ten times, and the average values are given in Table 1. The tribological tests were conducted on a UMT-3 ball-on-disk high-temperature tribometer (made by Bruker Corp., USA). The disk was the sintered material; before the test, the sintered material was cleaned with acetone and then dried in hot air. The counterpart ball was a commercial Al₂O₃ ceramic ball with a 10-mm diameter; the Al₂O₃ ball has a surface roughness of 0.032 μm , hardness of 16.5 GPa and density of 3.92 g cm^{-3} . The selected test temperatures of the friction and wear tests were RT, 300, 500, 700 and 900 °C. All the tests were run at a sliding velocity of 0.108 m s^{-1} , normal load of 20 N and duration of 60 min. The wear depth profiles of all the wear tracks were examined by a Nano Map 500LS contact surface mapping profiler (AEP Technology, USA) to obtain the wear rate of composites. The wear volume V was determined by the

following formula: $V = AP$, where A was the cross-sectional area of the worn scar and P was the perimeter of the worn scar. The wear rate was calculated as a function of the wear volume V divided by the sliding distance S and the applied load L and expressed as $\text{mm}^3 \text{ Nm}^{-1}$. All the tribological tests were carried out three times to assure the reproducibility of the experimental results in the same conditions, and the average results were reported.

3 Results

3.1 Hardness, Microstructure and XRD Analyses

The micro-hardness of the Ni-based composites is listed in Table 1. The hardness of the NCM composite was found to be the highest with a value of 319.35 HV. The NCA composite's hardness was the lowest (about 210 HV). The main reason was that Mo and MoO₃ can play a role in the enhancement function of the NiCr matrix. The hardness of the NCAMO composite was 285.55 HV and that of the NCAM composite 281.53 HV, slightly less than that of the NCAMO composite. The density of the composites was almost the same, except NCAMO, and the same added amount and almost the same density of Mo and Ag could have accounted for this. The density of NCAMO and NCAM composites was 7.85 and 8.27 g cm^{-3} , respectively; the difference in the density of the composites was attributed to the difference in the density between Mo (10.2 g cm^{-3}) and MoO₃ (4.69 g cm^{-3}).

Figure 1 shows the XRD patterns of the Ni-based composite before and after sintering. It can be seen that the Ni(Cr), Mo, MoO₃ and Ag phases can be identified from the mixed powders (Fig. 1a). After hot-pressing sintering, the phase compositions were almost unchanged for the NC, NCM, NCA and NCAM composite. However, the clear diffraction peaks of MoO₃ disappeared, and the peaks of the Ni-based solution, Cr₂O₃ and Ag peaks were evident in the NCAMO composite (Fig. 1b). Meanwhile, the diffraction peaks of Ag₂MoO₄ and NiCr₂O₄ appeared in the sintered composite. This means that some solid phase

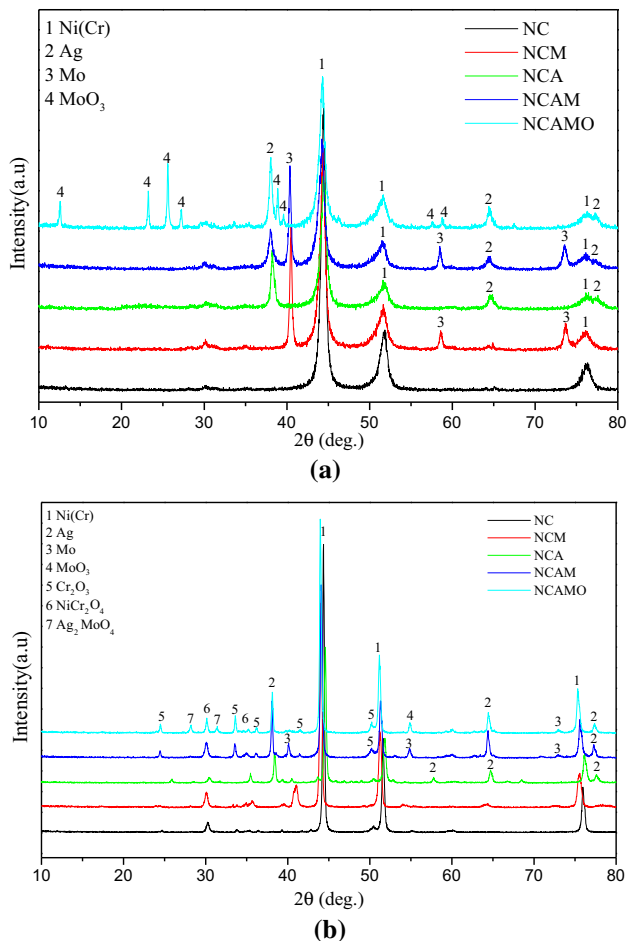


Fig. 1 XRD patterns of the Ni-based composites **a** before and **b** after hot-pressing

reactions happened during the sintering process. In addition, according to the XRD patterns of the NCM and NCAM composite (Fig. 1b), the Mo peaks became weaker than those before sintering (Fig. 1a) because some Mo solid dissolved in the Ni matrix during the high-temperature sintering process.

Figure 2 shows the typical microstructures of the Ni-based composites. The microstructure of these composites was quite dense, and there was only one phase in NC (Fig. 2a), two types of phase in both the NCM and NCA composites (Fig. 2b, c), and three types of phases in both the NCAM and NCAMO composites (Fig. 2d, e). Combining with EDS analysis revealed that the gray area was rich in Ni and Cr phases; the deep gray region was rich in Mo, Cr, Ni and O phases, while the white area was rich in the Ag phase. Besides, the Mo phase was observed to be distributed uniformly in the Ni(Cr) matrix (Fig. 2b, d), and the Ag phase dispersed in the matrix in a single phase and almost have not formed a solution in the Ni(Cr) matrix (Fig. 2c, d).

3.2 Tribological Properties of the Composites

Figure 3 gives the tribological properties of the Ni-based composite sliding against alumina balls at different temperatures. It can be seen that NC recorded the highest friction coefficient (the lowest value is about 0.4 at 900 °C) and wear rate ($>1 \times 10^{-4} \text{ mm}^3 \text{ N}^{-1} \text{ m}^{-1}$) (Fig. 3a, b) in these composites in the whole temperature range. Therefore, the common NiCr alloy did not have lubricity. When Mo or Ag was added to the NiCr matrix, the tribological performance of the composites had a certain degree of improvement. Both the NCM and NCA composite friction coefficients reached about 0.3, and the wear rates were about $5 \times 10^{-5} \text{ mm}^3 \text{ N}^{-1} \text{ m}^{-1}$ at high temperature. However, the tribological performance was still poor when the temperature was below 500 °C according to Fig. 3. When the combinations of Ag and (Mo or MoO₃) were added to the NiCr matrix, the tribological performance of the composites was significantly improved, especially at high temperatures. It can be seen that the friction coefficient of the NCAMO composite constantly decreased with increasing temperature and the lowest friction coefficient reached 0.19 at 900 °C (Fig. 3a). Likewise, the friction coefficient of the NCAM composite decreased with the temperature increasing to 700 °C; the minimum was about 0.23. However, the friction coefficient was then slightly increased to about 0.28 at 900 °C. Moreover, the wear rate of the NCAMO composite was relatively high at room temperature and about $22.7 \times 10^{-5} \text{ mm}^3 \text{ N}^{-1} \text{ m}^{-1}$ (Fig. 3b), but the wear rate of the NCAM composite at room temperature was moderate and around $9.22 \times 10^{-5} \text{ mm}^3 \text{ N}^{-1} \text{ m}^{-1}$. The wear rate of the NCAMO composite was found to decrease continuously with increasing temperature, and the lowest wear rate was registered at about $4.68 \times 10^{-6} \text{ mm}^3 \text{ N}^{-1} \text{ m}^{-1}$ at 900 °C. Similarly, the wear rate of the NCAM composite decreased with increasing temperatures up to 700 °C; the lowest wear rate was reached at $1.35 \times 10^{-5} \text{ mm}^3 \text{ N}^{-1} \text{ m}^{-1}$, while the wear rate value increased to $4.80 \times 10^{-5} \text{ mm}^3 \text{ N}^{-1} \text{ m}^{-1}$ when the temperature increased to 900 °C. Interestingly, the wear rate of the NCAMO composite was higher than that of the NCAM composite when testing temperatures below 700 °C, while the NCAMO composite had a favorable wear rate when temperatures were above 700 °C and was lower than that of the NCAM composite.

Figure 4 presents the typical variations of the friction coefficient of the NC, NCM, NCA, NCAM and NCAMO composites with sliding duration at elevated temperatures. The friction coefficient of the NCM and NCAM composites rapidly reached steady state in a shorter sliding time at each temperature, and the running-up duration was shorter with the temperature increases compared with other composites (Fig. 4b, d). However, the composites without

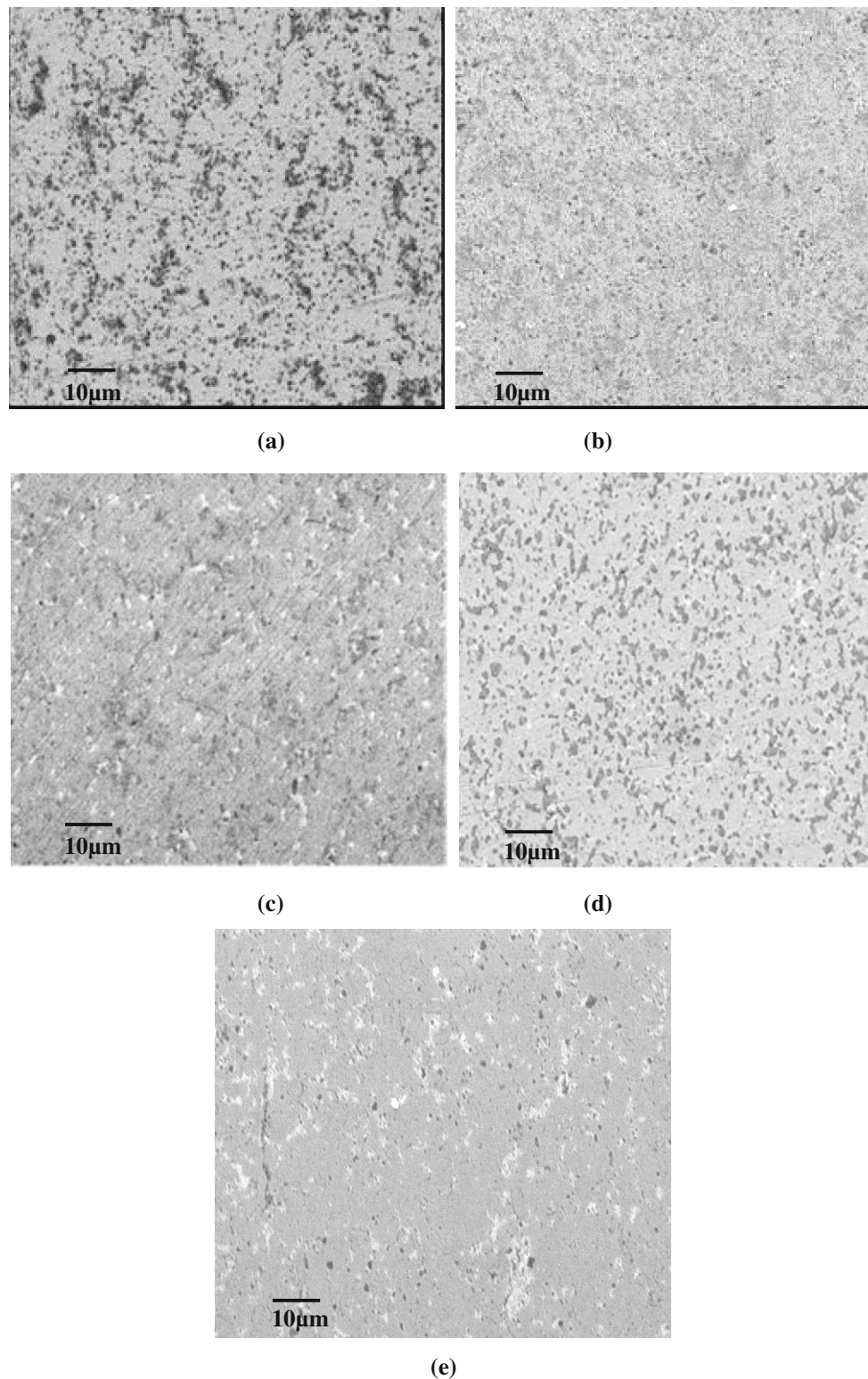


Fig. 2 SEM micrographs of the **a** NiCr; **b** NiCr-10Mo; **c** NiCr-10Ag; **d** NiCr-10Mo-10Ag; **e** NiCr-10MoO₃-10Ag composites

molybdenum (NC, NCA and NCAMO) displayed diverse running-up periods (Fig. 4a, c, e); this might be because the thermo-mechanical effects took place at the tribocontact

region, leading to a long running-up period. In addition, at room temperature and 300 °C, the friction coefficient of the NCAM composite was about 0.47 after the running-up

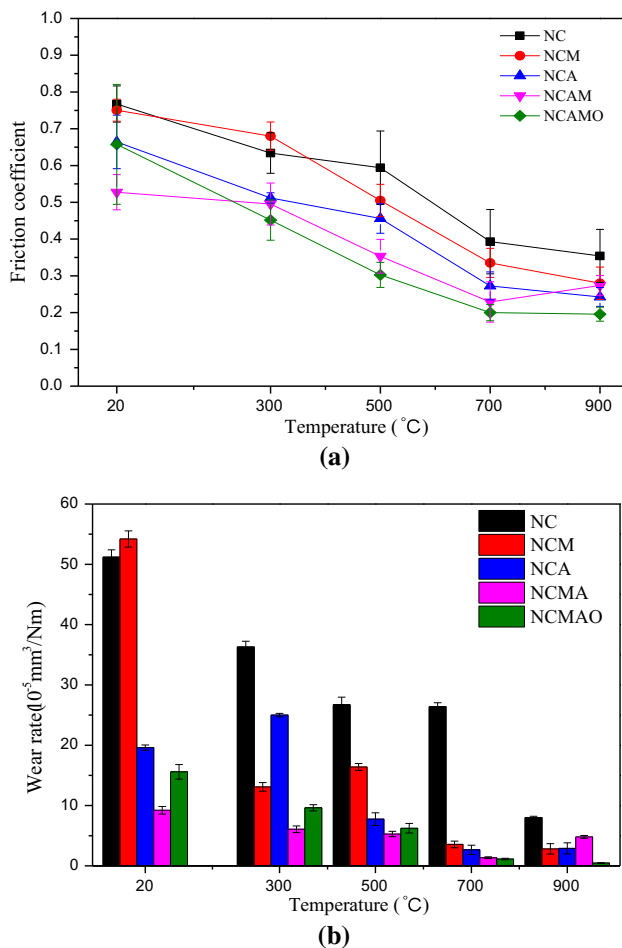


Fig. 3 Tribological properties of the Ni-based composites sliding against alumina balls at different temperatures (0.108 m s^{-1} , 20 N and 60 min): **a** friction coefficient; **b** wear rate

duration. As the temperature increased to 500 and 900 °C, the variation trend of the friction coefficient was the same, and the steady-state friction coefficient was 0.32 and 0.18, respectively. However, at 700 °C, the friction coefficient markedly decreased at first and then increased; the final friction coefficient at steady state was about 0.30. The friction coefficient of the NCAMO composite with sliding duration at room temperature was relatively high (about 0.7) and also had some fluctuations. With increasing temperature, the variation trend of the friction coefficient with sliding duration was almost the same; the friction coefficient decreased at first then achieved stability at each temperature test point. At 300 °C, the value at steady state was about 0.45, and 0.25 at 500 °C. When the temperature increased to 700 and 900 °C, a relatively smooth $F-t$ curve could be obtained, and the lowest friction coefficient was approximately 0.19.

In general, according to the results shown in Figs. 3 and 4, the NCAM and NCAMO composites displayed better

tribological properties compared with other composites at high temperatures.

3.3 SEM Morphologies of the Worn Surfaces of the Composites at Different Temperatures

Figure 5 gives the SEM morphologies of the worn surfaces of the Ni-based composites from room temperature to 900 °C. At room temperature, the worn surfaces of the NC, NCM and NCAMO composite covered a large number of wear debris particles (Fig. 5a). This was due to the severe abrasive action between the tribological pairs of the composites disk and alumina ball, and the wear mechanism was dominated by abrasive wear. Therefore, the wear rate of these composites was high at room temperature (Fig. 3b). The worn surfaces of the NCA and NCAM composite are found to have little wear debris and few delamination pits and few grooves on the worn surfaces, which illustrates that the wear mechanism is mainly delamination and microplowing (Fig. 5a). As the temperature increased to 300 °C, plastic deformation and some wear debris could be observed on the worn surface of NC, NCM and NCA composites and some flaky wear debris, and fine grooves appeared on the worn scar of the NCAMO composite and indicated that the wear mechanisms were characterized by delamination and microplowing (Fig. 5b). At 300 °C, many grooves and a deformed surface appeared on the worn surface of the NCAM composite, suggesting that the wear mechanisms were microplowing and surface plastic deformation. At 500 °C, the plastic deformation and many fine grooves on the worn surface of the NC, NCM and NCA composites could be clearly observed, and the worn surface became relatively smooth. Moreover, some wear debris could also be observed on the worn surface of NC and NCM composites (Fig. 5c). Therefore, the friction coefficient and wear rate were still high at this temperature. At 500 °C, a severely deformed surface appeared, and a few fine grooves could be seen on the worn surface of the NCAMO composite, suggesting that the wear mechanism is dominated by microplowing and surface plastic deformation (Fig. 5c). In addition, a smooth tribo-film covered the worn surface of the NCAM composite, and the worn surfaces were getting quite smooth, so the tribological properties were better than in the NC, NCM and NCA composites at 500 °C. As the temperature increased to 700 °C, the worn surfaces of all the composites except for NC (its worn surface was not smooth and had some delamination) were covered by a smooth tribo-film, implying the tribochemical reactions had taken place (Fig. 5d), and these composites almost showed the best tribological properties at this temperature. When the temperature reached 900 °C, by comparison with the SEM image at 700 °C, the smooth film almost completely

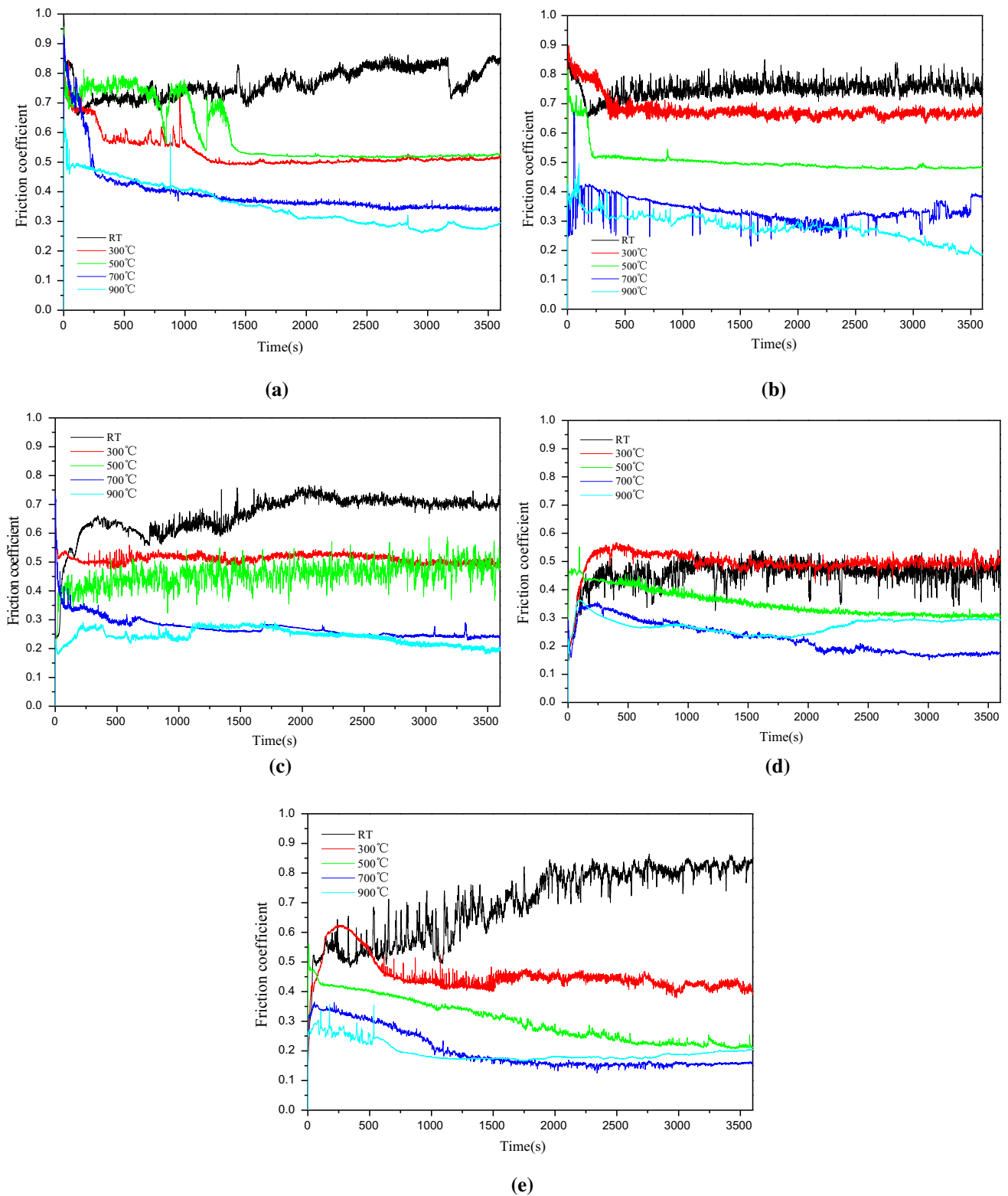


Fig. 4 Variation of the friction coefficient of the composites versus sliding duration under a normal load of 20 N and a sliding speed of 0.108 m s^{-1} from room temperature to $900 \text{ }^\circ\text{C}$: **a** NiCr, **b** NiCr-

10Mo, **c** NiCr-10Ag, **d** NiCr-10Mo-10Ag and **e** NiCr-10MoO₃-10Ag composites

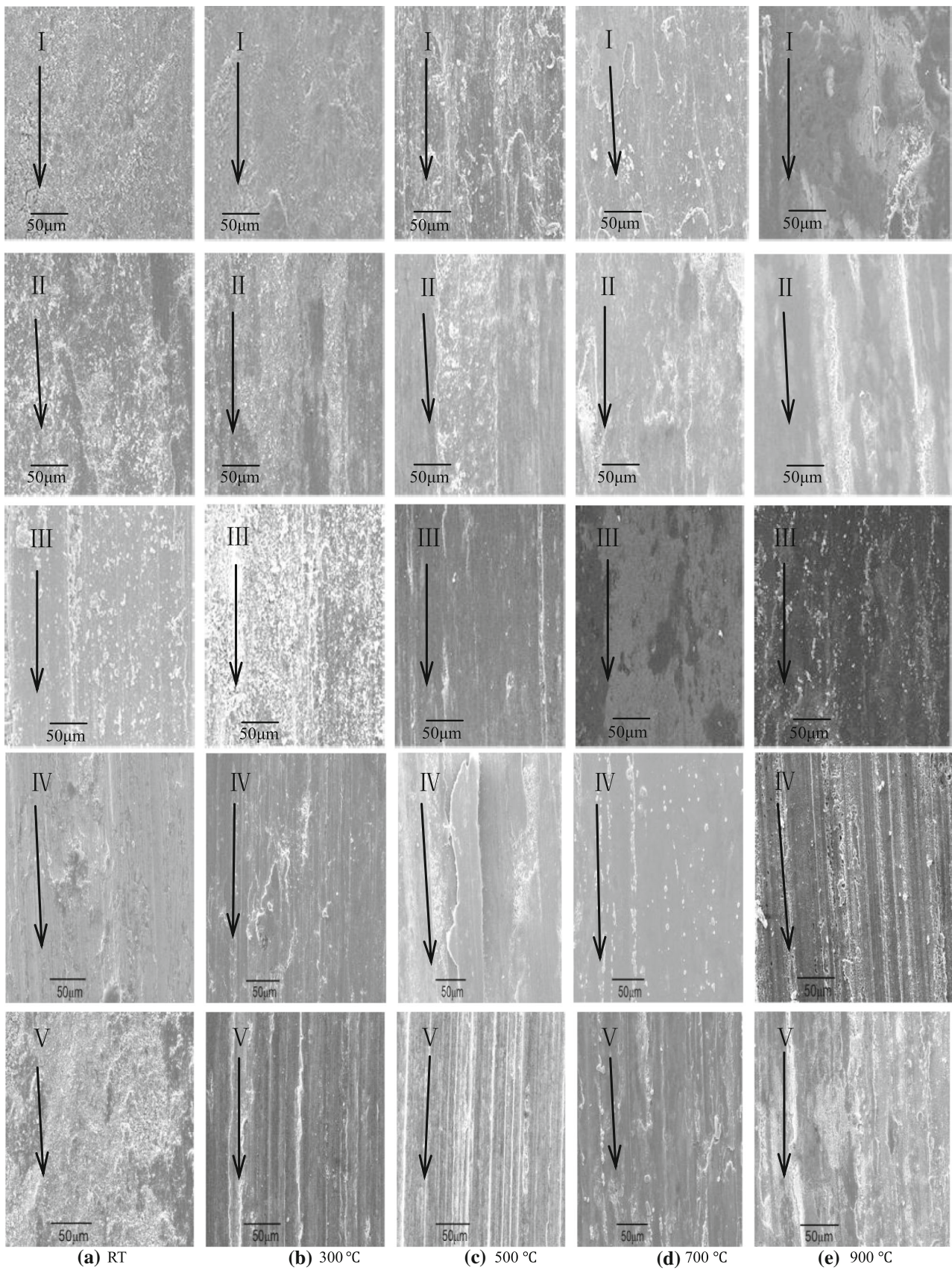
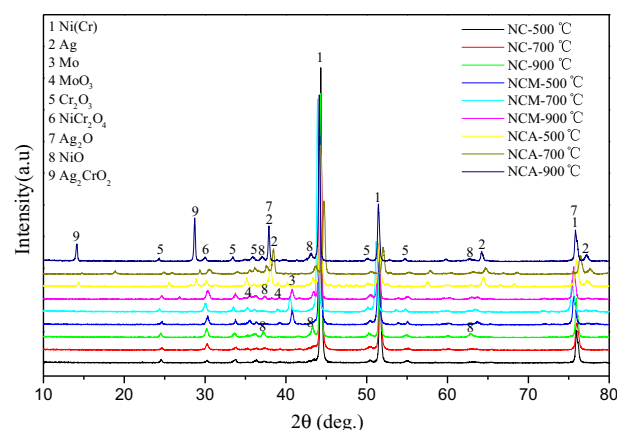


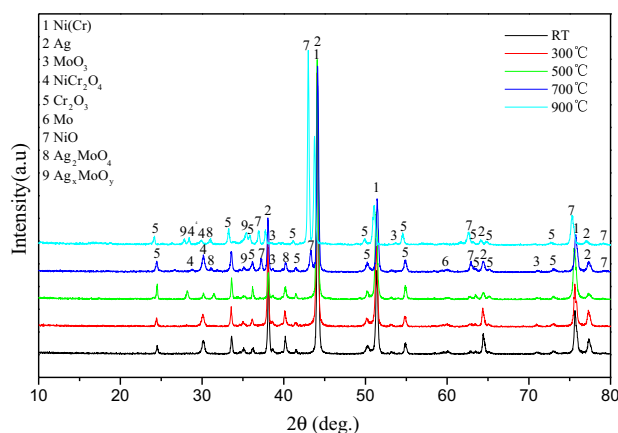
Fig. 5 SEM micrographs of the worn surfaces of (I) NiCr, (II) NiCr-10Mo, (III) NiCr-10Ag, (IV) NiCr-10Ag-10Mo and (V) NiCr-10Ag-10Mo₃ composites tested at different temperatures: **a** room temperature, **b** 300 °C, **c** 500 °C, **d** 700 °C, **e** 900 °C

covered the worn surface of all the composites (Fig. 5e), and the friction coefficient and wear rate of these composites presented very low values. In addition, it was clearly observed that silver precipitation from the worn surface of NCA and NCAM composites at 700 °C according to the EDS analysis (Fig. 5d, e) and both composites presented a very low friction coefficient and wear rate; this was attributed to increasing Ag diffusing to the worn surface to form lubricious surface aggregates with test temperature growth to about 700 °C [27, 28]. Furthermore, at 900 °C, the integrity of tribofilms on the worn surface of NCAM was damaged, and the worn surfaces became incomplete (Fig. 5e). Therefore, the wear rate of the NCAM composite at 900 °C was relatively higher than that at 700 °C.

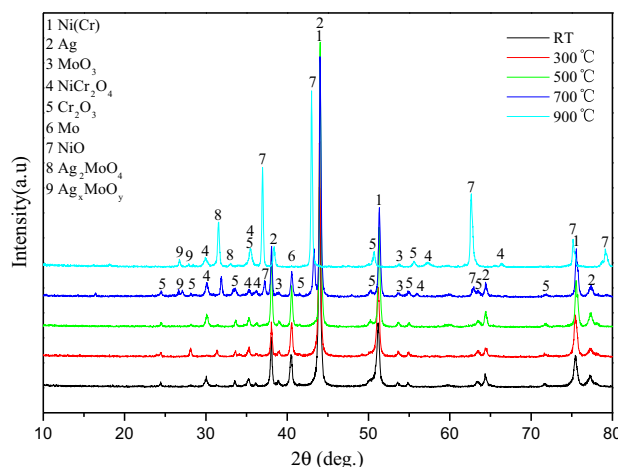
Figure 6 shows the XRD patterns of NC, NCM, NCA, NCAM and NCAMO composites after the wear test at different temperatures. According to the XRD patterns of NC, NCM and NCA composites shown in Fig. 6a, it could be seen that the diffraction peaks of the NiCr solution, Cr₂O₃ and NiCr₂O₄ were identified on the worn surfaces of NC below 700 °C. When the temperature reached 900 °C, the NiO diffraction peaks appeared on the worn surfaces of NC. NC showed very poor tribological properties; this was due to NiO and NiCr₂O₄ providing limited lubricity and no lubrication at low temperature (<500 °C), which was in agreement with previous reports [29]. It could be seen that the diffraction peaks of NiCr solution, MoO₃, Cr₂O₃ and NiCr₂O₄ were identified on the worn surfaces of the NCM composite below 700 °C; furthermore, the diffraction peaks of NiO were identified on the worn surfaces at 900 °C. The MoO₃ and NiO were the new phases compared with sintered NCM, so MoO₃ and NiO played the important role of lubricants at high temperature for NCM composites. It could also be found that the diffraction peaks of the NiCr solution, Cr₂O₃, Ag, Ag₂O and NiCr₂O₄ were identified on the worn surfaces of the NCA composite below 700 °C, so Ag played the main role in lubrication below 700 °C. Furthermore, diffraction peaks of NiO, Ag₂CrO₂ and Ag₂O were identified on the worn surfaces at 900 °C; together with Ag they worked synergistically to improve the tribological properties of the NCA composite. According to the XRD patterns of the NCAM and NCAMO composites shown in Fig. 6b, c, the diffraction peaks of the NiCr solution, MoO₃, Cr₂O₃, Ag, Ag₂MoO₄ and NiCr₂O₄ were identified on the worn surfaces of the NCAMO composite below 700 °C, while at 900 °C, the diffraction



(a)



(b)



(c)

Fig. 6 XRD patterns of **a** NiCr, NiCr-10Mo and NiCr-10Ag composites after the tribological property test at elevated temperatures; **b** NiCr-10Ag-10Mo₃ and **c** NiCr-10Ag-10Mo composites after tribological property tests from room temperature to 900 °C

peaks of Ag became feeble; the Ag₂MoO₄ and NiO peaks were getting stronger and sharper on the worn surfaces of the composite than those at 700 °C (Fig. 6b). As to the

NCAM composite, the diffraction peaks of the NiCr solution, Mo, Cr_2O_3 , Ag and NiCr_2O_4 were clearly identified on the worn surfaces below 700 °C (Fig. 6c); the diffraction peaks of NiO were also identified on the worn surfaces at 700 °C. Besides, the diffraction peaks of Ag_2MoO_4 appeared at 700 °C, and both of the diffraction peaks of NiO and Ag_2MoO_4 became sharper at 900 °C. The new compounds Ag_2MoO_4 and Ag_xMoO_y might have formed on the worn surface because of the tribo-chemical reactions among Ag, Mo and O at high temperatures. The Mo and Ag phases were identified on the worn surface of the NCAM composite and NCAMO composite at test temperatures below 700 °C, while at 900 °C, the diffraction peaks of Mo almost disappeared and the intensities of Ag peaks dramatically decreased.

Figures 7 and 8 display elemental composition mappings of the worn surfaces of the NiCr–10Mo and NiCr–10Ag composites at elevated temperatures, respectively. Silver was clearly detected to increase on the wear scars at all test temperatures, but the detection of molybdenum did not show evident changes. The main reason for this difference was the low melting point of silver and faster diffusion rate at higher temperatures [21]. The EDS analysis of the worn surfaces of the NiCr–10Mo and NiCr–

10Ag composites at elevated temperatures is further given in Tables 2 and 3, respectively. The weight percentages of silver on the rubbing surface of the NiCr–10Ag composite showed a gradual increase with increasing temperature, and the weight percentages of silver on the rubbing surface of NiCr–10Mo molybdenum declined rather than increased. Besides, it was quite certain that the oxidation resistance of NiCr–10Mo was higher than that of NiCr–10Ag based on the weight percentages of oxygen given in Tables 2 and 3.

3.4 Raman Analysis of the Wear Tracks of NCAM and NCAMO Composites

In order to further study the tribo-chemical changes on the worn surfaces of the NCAMO and NCAM composite at high temperatures, micro-Raman analysis was conducted. Figures 9 and 10 give the Raman spectra of the worn surfaces as well as the unworn surfaces of the NCAMO and NCAM composites from 500 to 900 °C, respectively. Very weak Ag_2MoO_4 and other compound peaks appeared for the Raman spectrum of the NCAMO composite after friction tests at 500 °C, which agreed well with the XRD results (Fig. 9a). When the temperature increased to 700 °C, clear Raman peaks of Ag_2MoO_4 appeared in the

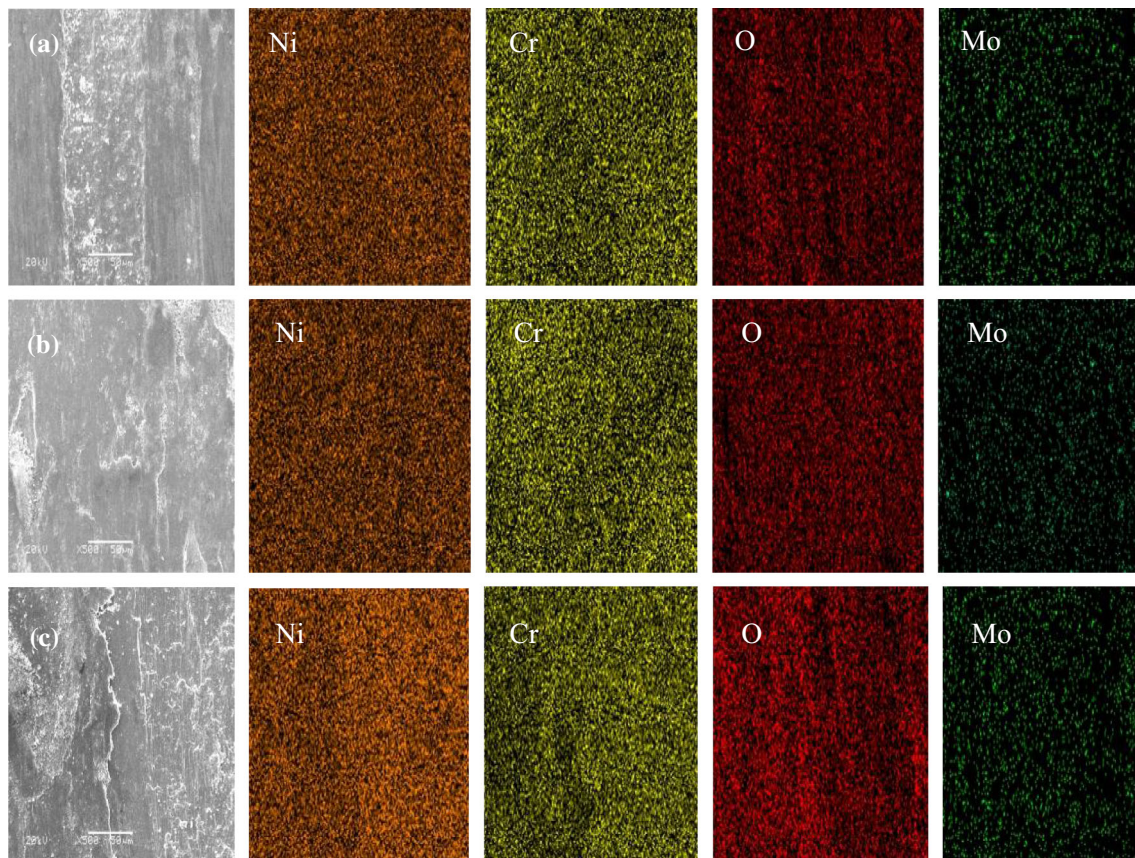


Fig. 7 Elemental composition mappings of the worn surfaces of the NiCr–10Mo composites: **a** 500 °C; **b** 700 °C; **c** 900 °C

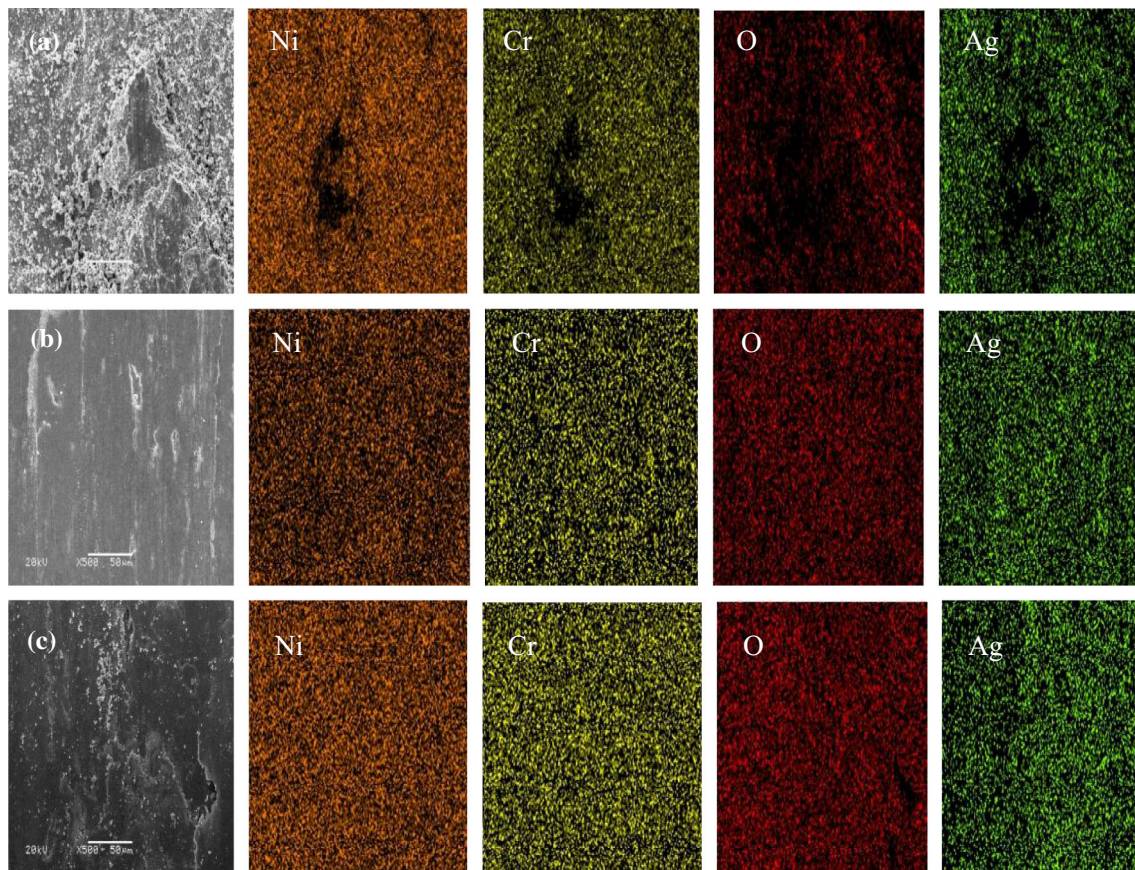


Fig. 8 Elemental composition mappings of the worn surfaces of the NiCr-10Ag composites: **a** 500 °C; **b** 700 °C; **c** 900 °C

Table 2 EDS analysis of the worn surfaces of the NiCr-10Mo composites at elevated temperatures

Temperature(°C)	Elemental composition (wt%)				
	Ni	Cr	O	Mo	Al
500	56.26	15.22	19.41	8.57	0.54
700	52.31	16.99	21.87	8.01	0.82
900	55.72	18.26	17.80	7.87	0.06

Table 3 EDS analysis of the worn surfaces of the NiCr-10Ag composites at elevated temperatures

Temperature(°C)	Elemental composition (wt%)				
	Ni	Cr	O	Ag	Al
500	54.98	14.60	23.71	6.25	0.46
700	50.21	13.15	28.34	7.87	0.43
900	46.47	12.28	31.30	9.28	0.57

Raman spectrum (Fig. 9b) and displayed a peak centering at 867 cm^{-1} , which belonged to the monoclinic silver molybdate phase [24, 26]. In addition, peaks of MoO_3 and Cr_2O_3 as well as NiO appeared. This result suggests that tribo-chemical reactions took place and new compounds formed with lubricating properties during the sliding process at high temperature [30, 31]. It is well known that molybdate is a kind of high-temperature lubricant that can provide a lubrication effect at high temperature. Therefore, the composite displayed the properties of low friction and wear at high temperatures. At 900 °C, besides the Raman peaks of Ag_2MoO_4 , the Raman peaks of $\text{Ag}_2\text{Mo}_4\text{O}_{13}$ appeared within the wear track (Fig. 9c). For the NC10AM composite, no slight Ag_2MoO_4 peaks appeared in the Raman spectra at a test temperature below 500 °C (Fig. 10a). This was different from the Raman spectrum of the NC10AMO composite. When the temperature increased to 700 °C, strong Raman peaks of Ag_2MoO_4 appeared (Fig. 10b), and $\text{Ag}_2\text{Mo}_4\text{O}_{13}$ could also be found from the Raman spectrum [32, 33]. At 900 °C, the peak of

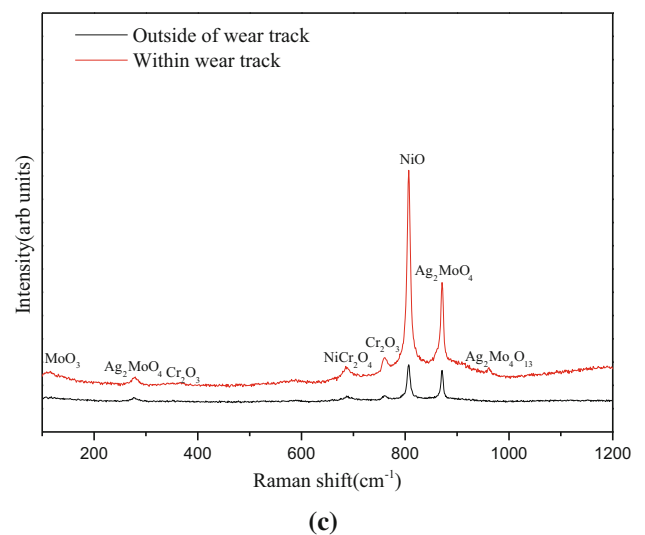
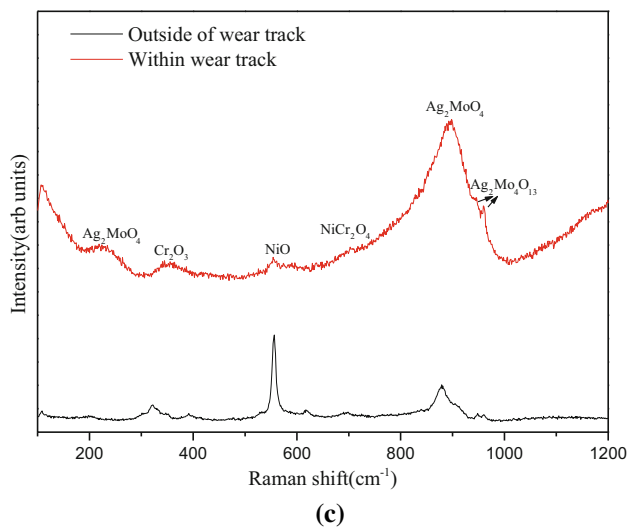
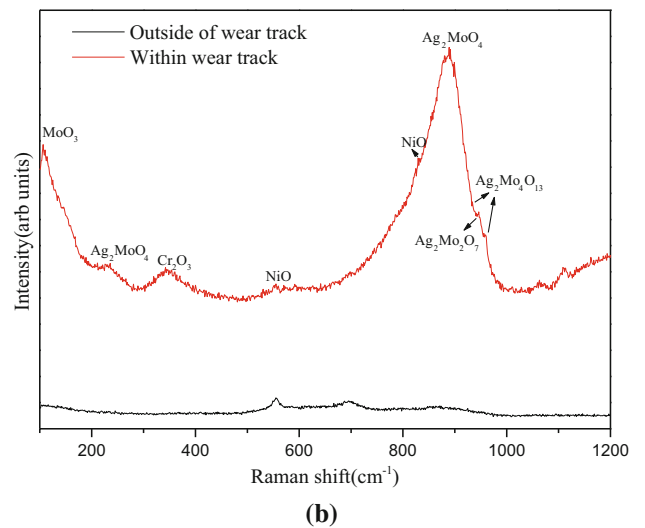
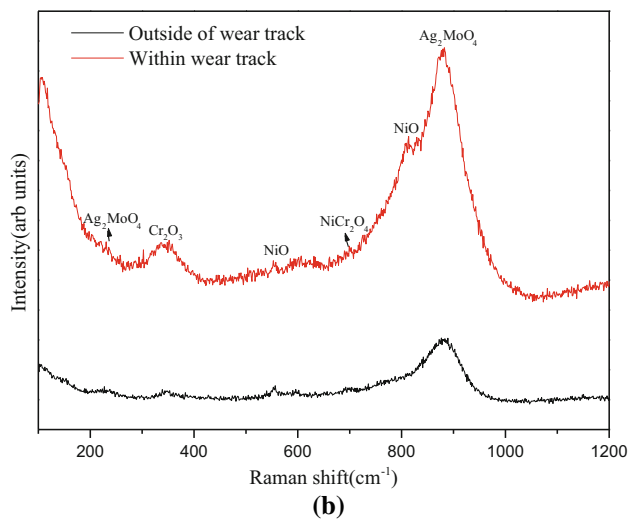
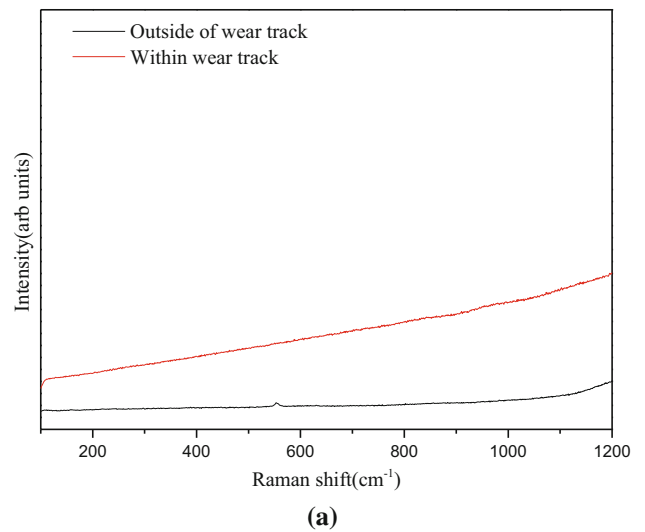
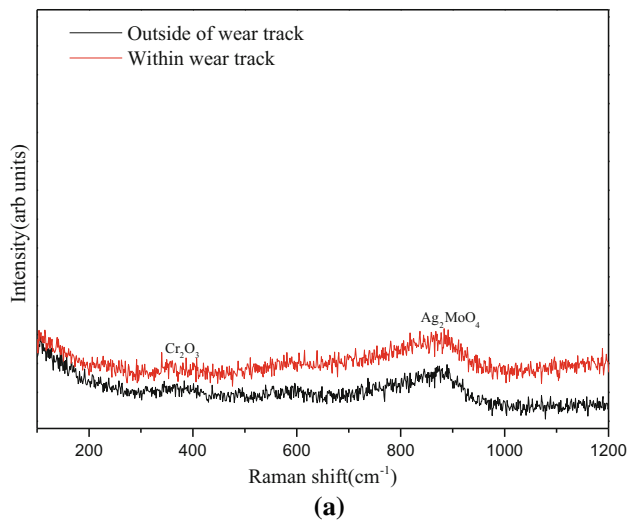


Fig. 9 Raman spectra of the NiCr-10Ag-10Mo₃ composite after testing at different temperatures: **a** 500 °C; **b** 700 °C; **c** 900 °C

Fig. 10 Raman spectra of the NiCr-10Ag-10Mo composite after testing at different temperatures: **a** 500 °C; **b** 700 °C; **c** 900 °C

NiO was shown brightly in the Raman spectrum (Fig. 9c). This was due to the severe oxidation that took place at high temperature.

For the purpose of further analyzing the glaze layer that formed on the worn surface of the NCAM and NCAMO composites after the wear test at high temperature, nanoindentation experiments were conducted to measure the mechanical properties of the glaze layer formed on the worn surface of the composites. Figure 11 presents the curves of the nanoindentation force versus penetration depth for the glaze layer of composites after wear tests at 700 and 900 °C, respectively. A tendency of the load-unload curves of the composites to be different was found, and the contact stiffness of the NCAMO composite at 700 and 900 °C was almost the same; however, the contact stiffness of the NCAMO composite at 700 and 900 °C was very different. This reflected the differences in the composites' resistance to the plastic deformation ability [34].

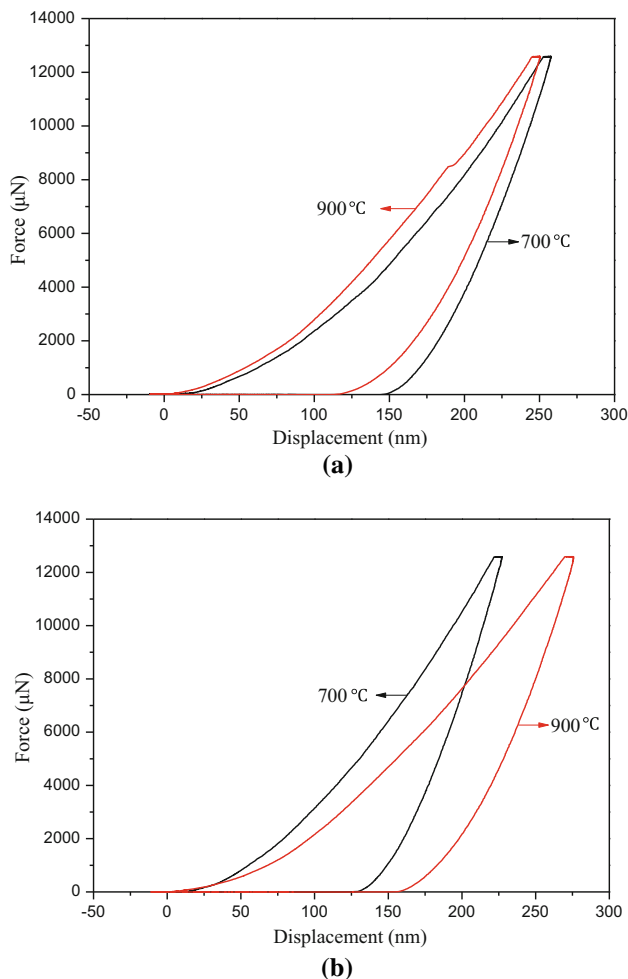


Fig. 11 Force versus penetration depth for the glaze layer on worn surfaces of **a** NiCr-10Ag-10Mo₃ and **b** NiCr-10Ag-10Mo after the wear test at 700 and 900 °C

The nano-hardness (H), Young's modulus (E) and the H/E ratio of the glaze layer on the worn surfaces of composites are given in Table 4. The H/E ratios have been reported to more accurately evaluate the anti-wear property of the composite than the hardness and higher H/E ratio as well as the good anti-wear property [35, 36]. The H/E ratio of the glaze layer of the NCAM composite was 0.065 at 700 °C and 0.089 at 900 °C, respectively, suggesting that the contact surface undergoes severe plastic deformation after high temperature wear and the worn surface is covered by a layer of lubrication film (Fig. 5d, e). This accounted for the wear rate of the NCAMO composite at 900 °C (on the order of $10^{-6} \text{ mm}^3 \text{ N}^{-1} \text{ m}^{-1}$). Moreover, the H/E ratios of the glaze layers of the two composites were almost the same at 700 °C, and their wear rate was quite comparable at 700 °C. The lowest H/E ratio of the glaze layer of the NCAM composite was at 900 °C (0.057), suggesting the higher wear rate of the NCAM composite, and obvious plastic deformation and adhesive wear were observed on the worn surfaces of the NCAM composite at 900 °C (Fig. 5e).

4 Discussion

It can be deduced that relatively good mechanical properties are necessary for Ni-based composites. The materials containing Mo have higher hardness than other materials, and the wear rate is relatively low. Furthermore, the friction coefficient rapidly reaches steady state in a shorter sliding time. The oxidation of metal molybdenum, which could form a MoO₃ lubricant film on the worn surface with the property of plastic deformation, and the further transfer to the surface of the coupled materials are believed to be the major reasons for the significant decrease in the friction coefficient at high temperatures [37]. However, when Ag is added to the composites, the mechanical properties of these composites deteriorate because Ag cannot provide the solution strength effect. On the basis of the experimental results, when Ag as a single lubricant was added to NiCr matrix, it did not significantly improve the tribological properties of the materials. This was attributed to the limitations of Ag itself (it only provides limited lubrication at a very narrow temperature range and has poor solid solubility) [8]. By combining two kinds of additives (Ag-MoO₃ or Ag-Mo), both of the composites displayed excellent tribological properties at high temperatures. Two aspects explain this: one is that the combination of two kinds of additives can meet the requirements of mechanical and lubricating performance at the same time; another is the change in the composition and contents of new phases during wear tests at high temperatures. The phases of NiCr₂O₄, Ag₂MoO₄ and Cr₂O₃ appear in the NCAMO

Table 4 Nano-hardness (H), Young's modulus (E) and H/E ratio of the glaze layer on the worn surfaces of NiCr–10Ag–10MoO₃ and NiCr–10Ag–10Mo composites after the wear test at 700 and 900 °C

Ni-based composites	Temperatures (°C)	Nano-hardness (H) (GPa)	Young's modulus (E) (GPa)	H/E
NC10AMO	700	8.82	134.89	0.065
	900	12.99	145.52	0.089
NC10AM	700	11.35	172.44	0.066
	900	7.31	128.61	0.057

composite after being hot pressed, and the composition and contents of these phases change during wear tests at high temperature according to the XRD results. At relatively low temperature (at RT), Ag₂MoO₄ cannot be easily sheared compared to Ag, and at the friction-contacted regions, cracks are initiated at first and then delamination occurs because of the low plasticity (Fig. 5a), which leads to the severe abrasive action of the NCAMO composite during the dry-sliding process. Therefore, the friction and wear properties are worse than for the NCAM composite. At high temperatures, the lubricating film, which is mainly composed of Ag₂MoO₄ and other oxides (Cr₂O₃ and NiO), is produced during the friction process according to XRD and Raman analysis. Within the wear track, clear Ag₂MoO₄ peaks are shown in the Raman patterns, and Ag₂MoO₄ as a solid lubricant is the predominant factor in the improvement of the tribological properties of the NCAMO and NCAM composites (Figs. 7b, 8b). A low friction coefficient and wear rate of the NCAMO and NCAM composites are displayed at high temperatures. In addition, at 700 and 900 °C, the low friction coefficient of the NCAMO composite is closely related to the synergistic work of Ag₂MoO₄, NiO and NiCr₂O₄, all of which have been found on worn surfaces according to XRD and Raman analysis. The high-temperature lubricious behavior of some molybdates and chromates has been studied, and the lubricity was found to be associated with low shear strength and high ductility at elevated temperatures [38–40].

The tribo-films composed of Ag₂MoO₄, NiO and NiCr₂O₄ and their contents are different according to the XRD and Raman spectrum results (shown in Figs. 6, 7, 8) and account for the difficulty degree of the formation and destruction of the transfer film. The low friction coefficient and wear rate of the NCAMO and NCAM composites from 300 to 700 °C are due to the change of the transfer film from the beginning, becoming complete and continuous. However, when the temperature increases to 900 °C, the ability to resist deforming of the NCAMO and NCAM composites is different, and compared with the NCAMO composite, the tribo-film formed on the worn surface of the NCAM composite is more easily destroyed. The worn surface morphologies from the relatively smooth surface to

the unsmooth surface (Fig. 5e) show the wear resistance of the NCAM composite weakened slightly, and a high wear rate is displayed.

In addition, the different compositions and contents of the tribo-films formed on the surface of the NCAMO composite and NCAM composite lead to the difference in the values of H , E and the ratio of H/E of the tribo-films that formed on the worn surface of the composites. According to the higher H/E ratio and better anti-wear property [37], the H/E ratios of the NCAMO composite at high temperatures are higher than those of the NCAM composite, and the tribological property of the NCAMO composite is better than that of the NCAM composite at high temperatures.

5 Conclusions

In this work, nickel-base composites containing Ag–MoO₃ or Ag–Mo were fabricated by the powder metallurgy technique, and the tribological properties of sliding against Al₂O₃ ceramic balls from room temperature to 900 °C were studied. In addition, for comparison, the materials of NiCr, NiCr–10Mo and NiCr–10Ag were also prepared and studied. The main conclusions can be drawn as follows:

1. Both composites show excellent tribological properties at high temperatures. The tribological properties of the composites are much more significantly improved by combining two kinds of additives (Ag–MoO₃ or Ag–Mo) than a single additive (Mo or Ag). As for the NCAMO composite, the corresponding lowest friction coefficient is about 0.19, and the lowest wear rate is about $4.68 \times 10^{-6} \text{ mm}^3 \text{ N}^{-1} \text{ m}^{-1}$. The lowest friction coefficient and wear rates of the NCAM composite are about 0.23 and $1.35 \times 10^{-5} \text{ mm}^3 \text{ N}^{-1} \text{ m}^{-1}$, respectively. The tribological properties of NCAMO and NCAM composites are better than NC and those composites with just only containing Ag or Mo, especially at high temperatures.
2. The difference in friction and wear properties between the composites is mainly due to the difference in the composition and contents of the tribo-layers, which consist of Ag₂MoO₄, NiCr₂O₄ and NiO formed on the worn surfaces of the composites during the sliding

process at high temperatures. The compound of Ag_2MoO_4 , NiCr_2O_4 and NiO on the worn surface works synergistically at high temperatures, which is the predominant factor leading to the improvement of the tribological properties of the composites.

3. The NiCr composites with only Mo or Ag do not have good comprehensive performance, but the Mo or MoO_3 additives can ensure the mechanical properties of the matrix. Moreover, combined with Ag they can provide excellent tribological properties of the composites for high temperature applications.
4. The wear mechanisms of the NCAMO composite are characterized by abrasion and micro-scuffing at low temperatures and by delamination, microploving and plastic deformation at high temperatures. The wear mechanisms of the NCAM composite are dominated by plastic deformation and delamination at low temperatures and delamination and plastic deformation at high temperatures.

Acknowledgments The authors acknowledge the financial support of the National Natural Science Foundation of China (Grant Nos. 50972148, 51471181, 51175490).

References

1. Spikes, H.: Tribology research in the twenty-first century. *Tribol. Int.* **34**, 789–799 (2001)
2. Zhao, J.C.: Ultrahigh-temperature materials for jet engines. *MRS Bull.* **28**, 620–630 (2003)
3. Donnet, C., Erdemir, A.: Historical developments and new trends in tribological and solid lubricant coatings. *Surf. Coat. Technol.* **180**, 76–84 (2004)
4. Aouadi, S.M., Singh, D.P., Stone, D.S., Polychronopoulou, K., Nahif, F., Rebholz, C., Muratore, C., Voevodin, A.A.: Adaptive VN/Ag nanocomposite coatings with lubricious behavior from 25 to 1000 °C. *Acta Mater.* **58**, 5326–5331 (2010)
5. Peterson, M., Li, S., Murray, S.: Wear-resisting oxide films for 900 °C. *J. Mater. Sci. Technol. (China)* **13**, 99–106 (1997)
6. Sliney, H.E.: Solid lubricant materials for high temperatures—a review. *Tribol. Int.* **15**, 303–315 (1982)
7. Xue, Q.J., Lu, J.J.: Research status and developing trend of solid lubrication at high temperatures. *Tribology* **19**(1), 91–96 (1999). (in Chinese)
8. Muratore, C., Voevodin, A.A., Hu, J.J., Jones, J.G., Zabinski, J.S.: Growth and characterization of nanocomposite yttria-stabilized zirconia with Ag and Mo. *Surf. Coat. Technol.* **200**, 1549–1554 (2005)
9. Xiong, D.S.: Lubrication behavior of Ni–Cr based alloys containing MoS_2 at high temperature. *Wear* **251**, 1094–1099 (2001)
10. Li, J.L., Xiong, D.S.: Tribological properties of nickel-based self-lubricating composite at elevated temperature and counterface material selection. *Wear* **265**, 533–539 (2008)
11. Li, J.L., Xiong, D.S., Huang, Z.J., Kong, J., Dai, J.H.: Effect of Ag and CeO_2 on friction and wear properties of Ni-base composite at high temperature. *Wear* **267**, 576–584 (2009)
12. Tyagi, R., Xiong, D.S., Li, J.L., Dai, J.: High-temperature friction and wear of Ag/h-BN-containing Ni-based composites against steel. *Tribol. Lett.* **40**, 181–186 (2010)
13. Chen, J.M., Hou, G.L., Chen, J., An, Y.L., Zhou, H.D., Zhao, X.Q., Yang, J.: Composition versus friction and wear behavior of plasma sprayed WC–(W, Cr)(2)C–Ni/Ag/BaF2–CaF2 self-lubricating composite coatings for use up to 600 °C. *Appl. Surf. Sci.* **261**, 584–592 (2012)
14. Liu, E., Gao, Y., Jia, J., Bai, Y.: Friction and wear behaviors of Ni-based composites containing graphite/ Ag_2MoO_4 lubricants. *Tribol. Lett.* **50**, 313–322 (2013)
15. Sliney, H.E., Dellacorte, C., Lukaszewicz, V.: The tribology of PS212 coatings and PM212 composites for the lubrication of titanium 6A1–4V components of a Stirling engine space power system. *Tribol. Trans.* **38**, 497–506 (1995)
16. DellaCorte, C., Laskowski, J.: Tribological evaluation of PS300: a new chrome oxide-based solid lubricant coating sliding against Al_2O_3 from 25 to 650 °C. *Tribol. Trans.* **40**, 163–167 (1997)
17. DellaCorte, C., Fellenstein, J.A.: The effect of compositional tailoring on the thermal expansion and tribological properties of PS300: a solid lubricant composite coating. *Tribol. Trans.* **40**, 639–642 (1997)
18. Blanchet, T.A., Kim, J.H., Calabrese, S.J., DellaCorte, C.: Thrust-washer evaluation of self-lubricating PS304 composite coatings in high temperature sliding contact. *Tribol. Trans.* **45**, 491–498 (2002)
19. DellaCorte, C., Edmonds, B.: NASA PS400: a new high temperature solid lubricant coating for high temperature wear applications. National Aeronautics and Space Administration, Glenn Research Center, Cleveland (2009)
20. Wahl, K., Seitzman, L., Bolster, R., Singer, I., Peterson, M.: Ion-beam deposited Cu–Mo coatings as high temperature solid lubricants. *Surf. Coat. Technol.* **89**, 245–251 (1997)
21. Chen, J., An, Y.L., Yang, J., Zhao, X.Q., Yan, F.Y., Zhou, H.D., Chen, J.M.: Tribological properties of adaptive NiCrAlY–Ag–Mo coatings prepared by atmospheric plasma spraying. *Surf. Coat. Technol.* **235**, 521–528 (2013)
22. Muratore, C., Voevodin, A.A., Hu, J.J., Zabinski, J.S.: Tribology of adaptive nanocomposite yttria-stabilized zirconia coatings containing silver and molybdenum from 25 to 700 °C. *Wear* **261**, 797–805 (2006)
23. Muratore, C., Voevodin, A.: Molybdenum disulfide as a lubricant and catalyst in adaptive nanocomposite coatings. *Surf. Coat. Technol.* **201**, 4125–4130 (2006)
24. Muratore, C., Bultman, J., Aouadi, S., Voevodin, A.: In situ Raman spectroscopy for examination of high temperature tribological processes. *Wear* **270**, 140–145 (2011)
25. Gulbinski, W., Suszko, T., Sienicki, W., Warcholiński, B.: Tribological properties of silver- and copper-doped transition metal oxide coatings. *Wear* **254**, 129–135 (2003)
26. Liu, E.Y., Wang, W.Z., Gao, Y.M., Jia, J.H.: Tribological properties of adaptive Ni-based composites with addition of lubricious Ag_2MoO_4 at elevated temperatures. *Tribol. Lett.* **47**, 21–30 (2012)
27. Mulligan, C.P., Blanchet, T.A., Gall, D.: CrN–Ag nanocomposite coatings: high-temperature tribological response. *Wear* **269**, 125–131 (2010)
28. Mulligan, C.P., Gall, D.: CrN–Ag self-lubricating hard coatings. *Surf. Coat. Technol.* **200**, 1495–1500 (2005)
29. Ouyang, J.H., Liang, X.S., Liu, Z.G., Yang, Z.L., Wang, Y.J.: Friction and wear properties of hot-pressed NiCr– BaCr_2O_4 high temperature self-lubricating composites. *Wear* **301**, 820–827 (2013)
30. Birks, N., Meier, G.H., Pettit, F.S.: Introduction to the high-temperature oxidation of metals, Chap. 5, 2nd edn. Cambridge University Press, New York (2006)
31. Basiev, T.T., Sobol, A.A., Voronko, Y.K., Zverev, P.G.: Spontaneous Raman spectroscopy of tungstate and molybdate crystals for Raman lasers. *Opt. Mater.* **15**, 205–216 (2000)
32. Aouadi, S.M., Paudel, Y., Luster, B., Stadler, S., Kohli, P., Muratore, C., Hager, C., Voevodin, A.A.: Adaptive $\text{Mo}_2\text{N}/\text{MoS}_2$

- Ag tribological nanocomposite coatings for aerospace applications. *Tribol. Lett.* **29**, 95–103 (2008)
33. Chen, F., Feng, Y., Shao, H., Zhang, X., Chen, J., Chen, N.: Friction and wear behaviors of Ag/MoS₂/G composite in different atmospheres and at different temperatures. *Tribol. Lett.* **47**, 139–148 (2012)
34. Li, J.L., Xiong, D.S., Wu, H.Y., Zhu, H.G., Kong, J., Tyagi, R.: Tribological properties of MoN layer on silver-containing nickel-base alloy at high temperatures. *Wear* **271**, 987–993 (2011)
35. Oliver, W.C., Pharr, G.M.: An improved technique for determining hardness and elastic modulus using load and displacement sensing indentation experiments. *J. Mater. Res.* **7**, 1564–1583 (1992)
36. Leyland, A., Matthews, A.: On the significance of the H/E ratio in wear control: a nanocomposite coating approach to optimised tribological behaviour. *Wear* **246**, 1–11 (2000)
37. Qi, Y.E., Zhang, Y.S., Hu, L.T.: High-temperature self-lubricated properties of Al₂O₃/Mo laminated composites. *Wear* **280–281**, 1–4 (2012)
38. Wu, X.Y., Du, J., Li, H.B., Zhang, M.F., Xi, B.J., Fan, H., Zhu, Y.C., Qian, Y.T.: Aqueous mineralization process to synthesize uniform shuttle-like BaMoO₄ microcrystals at room temperature. *J. Solid State Chem.* **180**, 3288–3295 (2007)
39. Gulbinski, W., Suszko, T.: Thin films of MoO₃–Ag₂O binary oxides—the high temperature lubricants. *Wear* **261**, 867–873 (2006)
40. Stone, D., Liu, J., Singh, D.P., Muratore, C., Voevodin, A.A., Mishra, S., Rebolz, C., Ge, Q., Aouadi, S.M.: Layered atomic structures of double oxides for low shear strength at high temperatures. *Scr. Mater.* **62**, 735–738 (2010)